Cesium Oxide Nanoparticles

Preparation and Structural Characterization of Stable Cs_2O Closed-Cage Structures**

*Ana Albu-Yaron, Talmon Arad, Ronit Popovitz-Biro, Maya Bar-Sadan, Yehiam Prior, Martin Jansen, and Reshef Tenne**

Films of cesium oxides with a Cs to O ratio of about 2:1 (in addition to Ag) and approximately monolayer dimensions are widely utilized, for example, on the surface of S-1 photocathodes,[1] negative electron affinity (NEA) devices,[2] and also discharge lamps, television cameras, and lasers. These films reduce the work function of the electrode and thereby increase the electron emission current and long-wavelength response of these devices.[1,2] Particular emphasis has been placed on the study of $Cs_{1+x}O$ for applications in catalytic converters[3,4] and optical fibers. The structure of these surface layers deposited on photoemissive and NEA devices has proved difficult to resolve and interpret, partly due to the thinness of the film and the pronounced instability of Cs_2O. Furthermore, as these films are highly reactive and thin, they are damaged or destroyed by short exposure to low vacuum. This stringent vacuum requirement increases the difficulty and expense of their manufacture and handling and prevents applications that require periodic atmospheric exposure. Enhancing the stability of these films is a long-standing goal.

The complex Cs–O phase diagram[5] has been investigated in the past. Although the synthesis of various oxides of cesium was reported already in the early 1900s, the actual structural characterization of Cs_2O and Cs_3O was described only 50 years later.[6,7] Cs_2O crystallizes in the 3R anti-$CdCl_2$ structure (PDF #09-0104)[8a,b] and is the only known binary alkali metal oxide with a layered structure. This suggests that a much more stable Cs_2O configuration should exist. Kinetic stabilization could be achieved by forming a closed-cage fullerene-like (*IF*) structure, which is the subject of the present report. These structures do not expose the highly reactive (*hk*0) prismatic faces, as the strong and reactive bonds of the cesium and oxygen atoms at the edges of the layers are canceled out by the inherently closed nature, and only rather weak interactions between adjacent Cs-O-Cs triple layers across the van der Waals gap actually occur. Moreover, *IF* including nanotubes[9] of various other layered compounds, such as WS_2[10,11] and BN,[12] were shown to have unusual mechanical, optical, and electronic properties that arise mainly from their highly curved surfaces, shape, and size. The extensive potential of WS_2 *IF* as superior solid lubricants[13] and impact-resistant materials[14] has already been confirmed.

Here we report the synthesis of closed-cage (fullerene-like *IF*) Cs_2O nanoparticles and their structural characterization by HRTEM. We attempted the synthesis using a variant of laser ablation in a rather unusual setup (Figure 1 a).

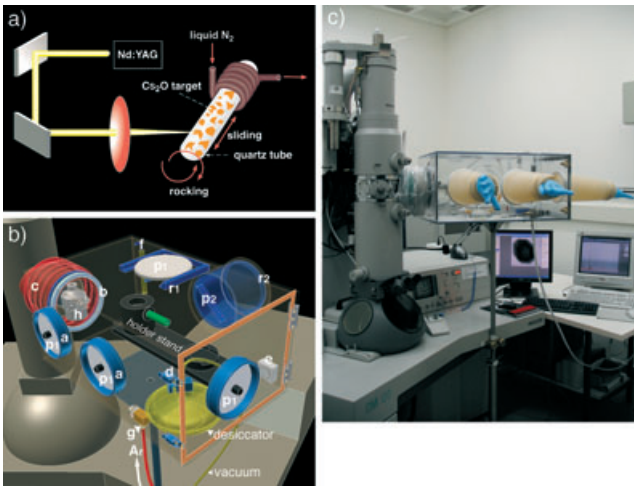

Figure 1. a) Experimental setup for laser ablation. b) Schematic of the environmental chamber. c) Image of the CM120 TEM with the environmental chamber attached to the CompuStage entry.

Moreover, a homebuilt argon-purged environmental chamber (Figure 1 b,c), tightly attached to the entry of the transmission electron microscope (TEM), has been designed and developed to overcome the tremendous experimental difficulties in manipulating Cs_2O. The synthesized nanoparticles exhibit remarkable stability not only under the electron beam of the microscope but also, to a certain extent, even when exposed temporarily to air, and this makes them potentially useful in developing new photoemissive and NEA devices.

3R-Cs_2O powder[15] (Figure 2) served as a precursor in the present work. Subsequent laser ablation of the powder while sealed in evacuated quartz ampoules led to the desired closed-cage nanoparticles of Cs_2O. Unfortunately, the production yields of the fullerene-like Cs_2O structures were too low to permit XRD characterization so far. Figure 3 a and b show two examples of closed-cage nested nanoparticles of Cs_2O typically observed in the laser-ablated material. While that shown in Figure 3 a is faceted, the layers of the *IF*-Cs_2O nanoparticles shown in Figure 3 b are evenly folded to form quasi-spherical, closed nanoparticles. Here, each fringe represents a molecular sheet of Cs_2O. The interlayer distance

[*] Dr. A. Albu-Yaron, Dr. R. Popovitz-Biro, M. Bar-Sadan, Prof. R. Tenne
Department of Materials and Interfaces
Weizmann Institute of Science
Rehovot 76100 (Israel)
Fax: (+972) 8-934-4138
E-mail: reshef.tenne@weizmann.ac.il
T. Arad
Electron Microscopy Unit
Weizmann Institute of Science
Rehovot 76100 (Israel)
Prof. Y. Prior
Department of Chemical Physics
Weizmann Institute of Science
Rehovot 76100 (Israel)
Prof. Dr. M. Jansen
Max-Planck-Institut für Festkörperforschung
Heisenbergstrasse 1, Stuttgart (Germany)

[**] The authors thank Mr. C. Mühle for the preparation of the samples.

 DOI: 10.1002/anie.200500356

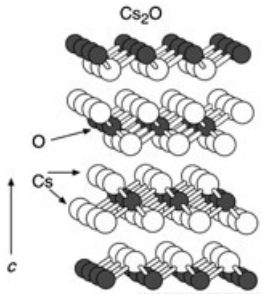

Figure 2. The structure of the Cs_2O precursor.

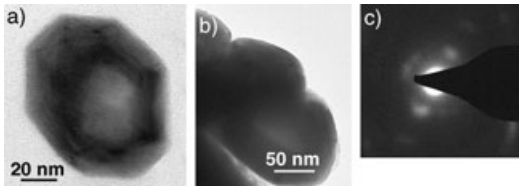

Figure 3. TEM images of typical closed-cage nested *IF*-Cs_2O nanoparticles obtained by laser ablation of 3R-Cs_2O powder precursor: a) faceted Cs_2O *IF* nanoparticle of approximately 70–90 nm in size, b) quasi-spherical *IF* nanoparticles of approximately 70–140 nm in diameter. All particles have at least 30 layers. c) SAED pattern of the nanoparticle in (a). Here reflections from both (00l) and (*hk*0) planes can be seen.

between the Cs_2O fringes is 6.35 Å. The faceted nanoparticle in Figure 3a is about 70–90 nm in size, while the quasi-spherical nanoparticles shown in Figure 3b are about 70–140 nm in diameter and consist of at least 30 layers. Although the nanoparticle cores appear quite dark, the somewhat brighter contrast suggests that they are hollow in the center. The folded and closed nature of both nanoparticles was verified by tilting experiments. Selected-area electron diffraction (SAED) from the nanoparticle in Figure 3a, which is shown in Figure 3c, exhibits the reflections of both (00l) and the hexagonal pattern of the (*hk*0) planes at any tilt angle and confirms the closed nature[10,11] of *IF*-CsO_2. Energy dispersive X-ray analysis (EDS) showed that only cesium and oxygen were present in the nanoparticle with an approximate 2:1 ratio.

Figure 4a shows an enlarged view of part of the faceted polyhedral Cs_2O nanoparticle shown in Figure 3a. A computer simulation of the magnified image is overlaid on the lattice image in Figure 4b. Note the good agreement between the simulated and experimentally observed image. A line profile of the framed area in Figure 4a, shown in Figure 4c, confirms the interlayer spacing of 6.37 Å, which agrees very well with the value of $^1/_3\,c$ of Cs_2O. The fast Fourier transform (FFT) of the framed region in Figure 4a is shown in Figure 4d, and the distance calculated therefrom (6.35 Å) also agrees with $^1/_3\,c$ of Cs_2O. The *IF*-Cs_2O nanoparticles were found to be very stable under the electron beam of the TEM, while TEM analysis of the surrounding amorphous or platelet bulk Cs_2O starting material, also present in these samples, was particularly difficult due to their instability and outgassing

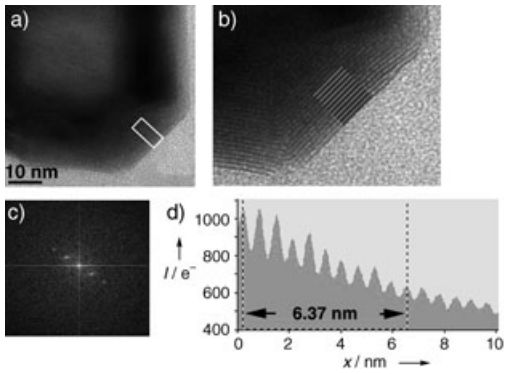

Figure 4. a) An enlarged view of part of a faceted Cs_2O nanoparticle. b) Higher magnification of the *IF*-Cs_2O nanoparticle displayed in a) with a computer simulation of the image overlaid on the lattice image. Note the good agreement between the simulated and experimentally observed images. c) FFT of the framed area in (a). d) Line profile of the framed area in (a) showing an interlayer spacing of 6.37 Å.

under the electron beam. More strikingly, when the grid bearing the specimen was taken out and reinserted into the TEM after a few minutes in the ambient atmosphere, almost no damage occurred to the inspected fullerene-like Cs_2O *IF* nanoparticles, while the surrounding Cs_2O material had deteriorated rapidly.

Subsequent HRTEM experiments on a grid transferred from the TEM and analyzed after roughly 1 h in the ambient laboratory atmosphere (Figure 5a), revealed that the pristine Cs_2O nanoparticle with fullerene-like structure was only partially damaged. The overall shape of this fullerene-like

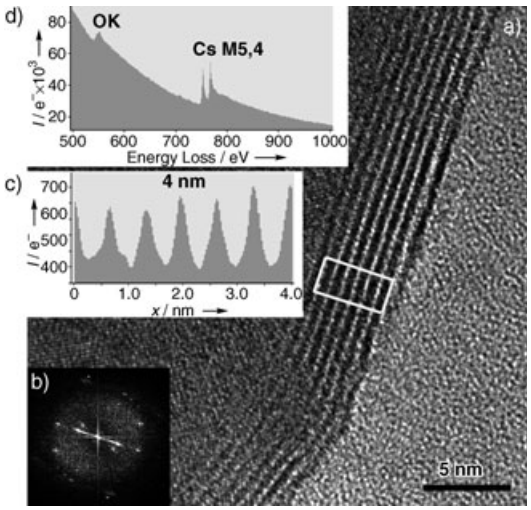

Figure 5. Higher magnification image of a faceted *IF*-Cs_2O nanoparticle, analyzed first in the CM120 TEM and then transferred to the HRTEM following about 1 h of exposure to ambient atmosphere. a) Region of the nanoparticle exhibiting reduced number of layers as compared to the 30 or more layers of a typical pristine nanoparticle (see Figures 3 and 4). The layer spacings, obtained from the respective FFT in (b) and the line profile in (c) from the framed areas in (a) is 6.8 Å in this part. The EELS spectrum in (d) exhibits only Cs and O in a ratio of less than 2:1.

nanoparticle changed from a faceted structure, like in Figure 3a, to a more spherical topology; starting from the kinks between the facets, exfoliation and amorphization of the outer molecular Cs_2O sheets took place and advanced progressively inwards. Careful inspection of this nanoparticle revealed that the number of perfectly closed molecular layers decreased from about 30 to 8, and most of the Cs_2O layers (ca. 20) were only partially ruptured. The interlayer distance increased from about 6.4 Å in the pristine nanoparticle to 6.8 Å (Figure 5b,c) and in some places even to 8.5 Å (not shown), likely due to intercalation of water. In general, however, the inner layers of the *IF*-Cs_2O nanoparticles were found to be undamaged and exhibited smaller expansion.

Electron energy loss spectroscopy (EELS) and imaging with the Gatan imaging filter (GIF) revealed only Cs and O (excess oxygen; Figure 5d), while GIF analysis of the surrounding amorphous material (not shown), revealed Cs, O, and C. These results, together with the above TEM observations, imply that the amorphous and platelet materials on the grid react vigorously with ambient CO_2 to form cesium carbonate, while the *IF* nanoparticles react slowly with water, which could be possibly removed by mild heat treatment or prolonged evacuation in the HRTEM column. In keeping with previous observations on alkali-metal-doped WS_2 and MoS_2 nanoparticles,[16] water uptake into the van der Waals gap between the layers is common in layered compounds. Furthermore, in analogy to intercalated *IF*-WS_2,[16] evidence for some time-dependent recovery of the damaged nanoparticles, accompanied by rounding of its initial polyhedral shape, was observed after a few days in the high vacuum of the HRTEM. The partially recovered Cs_2O layers were less faceted than the original ones. These observations indicate that, in contrast to the presently used cesium oxide films in photocathodes, which are irreversibly damaged under low vacuum, the *IF* nanoparticles, if damaged, could possibly be recovered by mild heating under vacuum.

The presence of the closed Cs-O-Cs hexagonal planes in the *IF*-Cs_2O structures clearly enhances the stability of the material in ambient atmosphere. The inert van der Waals surface of the closed nanoparticles presents a diffusion barrier to the intercalation process, which leads to a sequential and therefore slower hydrolytic attack on the layers in these structures. In contrast, the existence of dangling bonds at the prismatic edges on the periphery of the Cs_2O quasi-two-dimensional planar structures explains the high reactivity of amorphous or platelet powder. Therefore, the formation of closed-cage *IF*-Cs_2O nanostructures induces kinetic stabilization of the material and accounts for its intrinsically low reactivity.

The synthesis of *IF*-Cs_2O has led to a new member of the fullerene-like family of otherwise extremely unstable but important materials. The unprecedented relative stability of the *IF*-Cs_2O nanoparticles synthesized here, both under the electron beam and in air, is very encouraging and suggests that once larger amounts of pure *IF* nanoparticles have been synthesized and fully characterized, their beneficial effect on lowering the work function and photoemission from various surfaces could be directly evaluated and fully exploited in NEA, photoemissive, and other devices. The action of other metals, such as silver and bismuth, that are known to enhance the quantum yield of photocathodes may in fact be related to their possible catalytic effect in the synthesis of *IF*-Cs_2O nanoparticles. Theoretical work is underway to elucidate the electronic structure of these nanoparticles. Previous studies on various semiconducting nanotubes[17,18] indicated that while quantum-size effects are of lesser importance in closed-cage nanostructures, folding of the molecular sheets reduces the energy gap and makes the nanotubes more conductive, and this could favorably affect their thermionic and photoemission.

Experimental Section

The 3R-Cs_2O powder precursor in the present work was synthesized by reaction of measured amounts of cesium metal and oxygen at 180 °C for 3 d.[15] The product was subsequently sealed in evacuated quartz ampoules. The orange-tinted powder was characterized by XRD and Raman spectroscopy.[8a,b] The Raman peak at $\tilde{\nu} = 103\ cm^{-1}$ can be assigned to the A_{1g} mode.[8a]

Cs_2O powder precursor in a vacuum-sealed quartz ampoule was ablated with a pulsed Nd:YAG laser; the beam was manually scanned so as to impinge on a new position. Cooling with liquid N_2 vapor was performed through a copper tube in the form of a helical coil, which wrapped part of the ampoule surface. Figure 1a shows the experimental arrangement. During ablation, a deeply colored powder accumulated on the walls of the cooled side of the quartz ampoule.

Further manipulations were performed in a specially designed and built environmental cell attached as a matching counterpart to the CompuStage entry of the TEM, operating under a flow of Ar of purity > 99.99 % and without any modification of the microscope or of the sample holder; it allowed safe preparation, mounting, handling, and introduction into the microscope of the specimen grid without exposure to the ambient atmosphere. Figure 1b shows a schematic of the environmental chamber; Figure 1c is an overview of the installation of the chamber attached to the CM120 TEM column. The quartz ampoule was broken inside the chamber, and a small amount of the laser-ablated material transferred onto a gold grid for mounting into the TEM. The environmental chamber was operated with both the room-temperature and the cryo holders of the CM120 TEM. A completely different system, which only excludes air during insertion of the grid into the microscope, has been previously reported.[19]

The following microscopes were used: a TEM-Philips CM120 (120 kV) with EDS system (EDAX Phoenix) and a field-emission gun high-resolution TEM (HRTEM) model FEI Tecnai F-30 (300 kV). A Gatan imaging filter (GIF) was used for for electron energy loss spectroscopy (EELS) and for elemental mapping. Fast Fourier transform (FFT) of the high-resolution images was obtained by Digital Micrograph software (Gatan). The computer simulation was performed with the software MacTempas. The following parameters were used for the simulation: thickness 35 nm; defocus of −30 nm.

Received: January 30, 2005
Revised: March 22, 2005
Published online: June 3, 2005

Keywords: cage compounds · cesium · electron microscopy · nanostructures · oxides

[1] A. H. Sommer, *Photoemissive Materials*, Krieger, Huntington, **1980**, p. 132–166, pp. 167–174.
[2] W. E. Pickett, *Phys. Rev. Lett.* **1994**, *73*, 1664–1667.

[3] Z. You, I. Balint, K.-I. Aika, *Appl. Catal. B* **2004**, *53*, 233 – 244.
[4] B. A. A. L. van Setten, C. G. M. Spitters, J. Bremmer, A. M. M. Mulders, M. Makkee, J. A. Molijn, *Appl. Catal. B* **2003**, *42*, 337 – 347.
[5] A. Simon in *Structure and Bonding*, *Vol. 36* (Eds.: J. D. Dunitz, J. B. Goodenough, P. Hemmerich, J. A. Ibers, C. K. Jørgensen, J. B. Neilands, D. Reinem, R. G. P. Williams), Springer, New York, **1979**, pp. 81 – 127.
[6] K. R. Tsai, P. M. Harris, E. N. Lassettre, *J. Phys. Chem.* **1956**, *60*, 338 – 344.
[7] K. R. Tsai, P. M. Harris, E. N. Lassettre, *J. Phys. Chem.* **1956**, *60*, 345 – 347.
[8] a) A. Band, A. Albu-Yaron, T. Livne, H. Cohen, Y. Feldman, L. Shimon, R. Popovitz-Biro, V. Lyahovitskaya, R. Tenne, *J. Phys. Chem. B* **2004**, *108*, 12360 – 12367; b) S. Gemming, G. Seifert, C. Mühle, M. Jansen, A. Albu-Yaron, T. Arad, R. Tenne, *J. Solid State Chem.* **2005**, *178*, 1190 – 1196.
[9] C. N. R. Rao, M. Nath, *Dalton Trans.* **2003**, 1 – 25.
[10] R. Tenne, L. Margulis, M. Genut, G. Hodes, *Nature* **1992**, *360*, 444 – 446.
[11] L. Margulis, G. Salitra, R. Tenne, M. Talianker, *Nature* **1993**, *365*, 113 – 114.
[12] N. G. Chopra, J. Luyken, K. Cherry, V. H. Crespi, M. L. Cohen, S. G. Louie, A. Zettl, *Science* **1995**, *269*, 966 – 967.
[13] L. Rapoport, Yu. Bilik, Y. Feldman, M. Homyonfer, S. R. Cohen, R. Tenne, *Nature* **1997**,*387*, 791 – 793.
[14] Y. Q. Zhu, T. Sekine, K. S. Brigatti, S. Firth, R. Tenne, R. Rosentsveig, H. W. Kroto, D. R. M. Walton, *J. Am. Chem. Soc.* **2003**,*125*, 1329 – 1333.
[15] G. Brauer, *Handbuch der Präparativen Anorganischen Chemie*, *Vol. 2*, Enke, Stuttgart, **1978**, p. 938.
[16] A. Zak, Y. Feldman, V. Lyakhovitskaya, G. Leitus, R. Popovitz-Biro, E. Wachtel, H. Cohen, S. Reich, R. Tenne, *J. Am. Chem. Soc.* **2002**, *124*, 4747 – 4758.
[17] G. Seifert, H. Terrones, M. Terrones, M. Jungnickel, T. Frauenheim, *Phys. Rev. Lett.* **2000**, *85*, 146 – 149.
[18] I. Cabria, J. W. Mintmire, *Europhys. Lett.* **2004**, 65, 82 – 88.
[19] P. O. Jeitschko, A. Simon, R. Ramlau, Hj. Mattausch, *Z. Anorg. Allg. Chem.* **1997**, *623*, 1447 – 1454.

